



Evaluation of atlantooccipital overlapping and cerebral ventricle size in dogs with atlantoaxial instability

Fumitaka TAKAHASHI^{1,2)*}, Shigenori KOUNO¹⁾, Shinya YAMAGUCHI^{1,2)} and Yasushi HARA¹⁾

¹⁾The Laboratory of Veterinary Surgery, Nippon Veterinary and Life Science University, 1-7-1 Kyonan, Musashino-shi, Tokyo 180-0023, Japan

²⁾YPC Tokyo Animal Orthopedic Surgery Hospital, 7-1-13 Oojima, Koutou-ku, Tokyo 136-0072, Japan

ABSTRACT. This study investigated cerebral ventricle size and concurrent craniocervical junction abnormality in relation to atlantooccipital overlapping (AOO) in dogs with atlantoaxial instability (AAI). A total of 61 dogs were treated with atlantoaxial ventral fixation. Medical records of each dog, including magnetic resonance (MR) and computed tomography (CT) images, were retrospectively reviewed. CT images were assessed for the presence of AOO and the dogs were then assigned to either an AOO group or a non-AOO group accordingly. CT images were also evaluated to determine the foramen magnum (FM) index. Syringomyelia, cerebellar compression, dorsal compression, and the degree of enlargement of each cerebral ventricle were evaluated using MR images. Of the 61 dogs, 23 had AOO and 38 did not. Furthermore, the ventricle/brain height ratio, the fourth ventricle height/cerebellum length ratio, and the fourth ventricle width/cerebellum length ratio were significantly higher in the AOO group than in the non-AOO group. However, the FM index, third ventricle/brain height ratio, and incidence of syringomyelia did not differ significantly between the two groups. Dogs with concurrent AOO exhibited significantly more dilatation of the lateral and fourth ventricles.

KEY WORDS: atlantoaxial instability, atlantooccipital overlapping, cerebrospinal fluid, enlargement of the cerebral ventricle, syringomyelia

J. Vet. Med. Sci.

81(2): 229–236, 2019

doi: 10.1292/jvms.17-0553

Received: 12 October 2017

Accepted: 7 December 2018

Published online in J-STAGE:
24 December 2018

Atlantoaxial instability (AAI) is a group of disorders caused by congenital dysplasia in the areas from the occipital bone to the cranial cervical vertebrae (craniocervical junction abnormality [CJA]). The disease is common in young toy-breed dogs and leads to cervical spinal cord compression [2, 7–9, 12, 17, 19, 21, 26, 27, 34, 40, 44–46]. Although many studies have investigated the pathology of AAI using various techniques [2, 7, 9, 12, 17, 21, 27, 33, 34, 39, 40, 43–46], the pathology and causation of CJA remains poorly understood.

Basilar impression or basilar invagination (BI) is a human disease in which the arcus dorsalis of the atlas migrates to the rostral surface and invaginates toward the foramen magnum (FM), causing cerebellar compression (CC). BI is recognized as analogous to canine atlantooccipital overlapping (AOO) [3, 4, 28, 36] and studies have reported that, in humans, it may change blood flow through the basilar artery and cerebrospinal fluid (CSF) dynamics, potentially triggering syringomyelia [10, 23, 30, 35]. Human BI and canine AOO are recognized causes of compression of the caudal surface of the medulla oblongata, the cranial surface of the cervical spinal cord, and the cerebellomedullary cistern. AOO also causes indentations on the surface of the cerebellum [3, 4]. Disturbances in CSF circulation at the junction of the medulla oblongata and cervical spine have been implicated in the development of syringomyelia and hydrocephalus in dogs with CJA [3–5, 8].

When AAI in CJA results in subluxation of the atlantoaxial joint, sudden aggravation of clinical symptoms occurs and surgical intervention is preferentially required. In most cases of AAI, ventral fixation of the atlantoaxial joint results in a favorable prognosis [7, 43, 44]. In our previous study, the presence of AOO affected clinical signs but did not directly affect the outcome of surgical stabilization in dogs with AAI [43]. However, in cases with no improvement or worsening of neurological status or postoperative death, concurrent CJA pathology is suspected. Because simultaneously evaluating the cause of various CJA is difficult, the present study was focused on investigating cerebral ventricle size in dogs with AAI with and without AOO. The purpose of the current study was to compare the cerebral ventricle size and concurrence of CJA, which seem to be related to AOO, between dogs with AAI with and without AOO.

*Correspondence to: Takahashi, F.: takataka.pc1138@gmail.com

©2019 The Japanese Society of Veterinary Science



This is an open-access article distributed under the terms of the Creative Commons Attribution Non-Commercial No Derivatives (by-nc-nd) License. (CC-BY-NC-ND 4.0: <https://creativecommons.org/licenses/by-nc-nd/4.0/>)

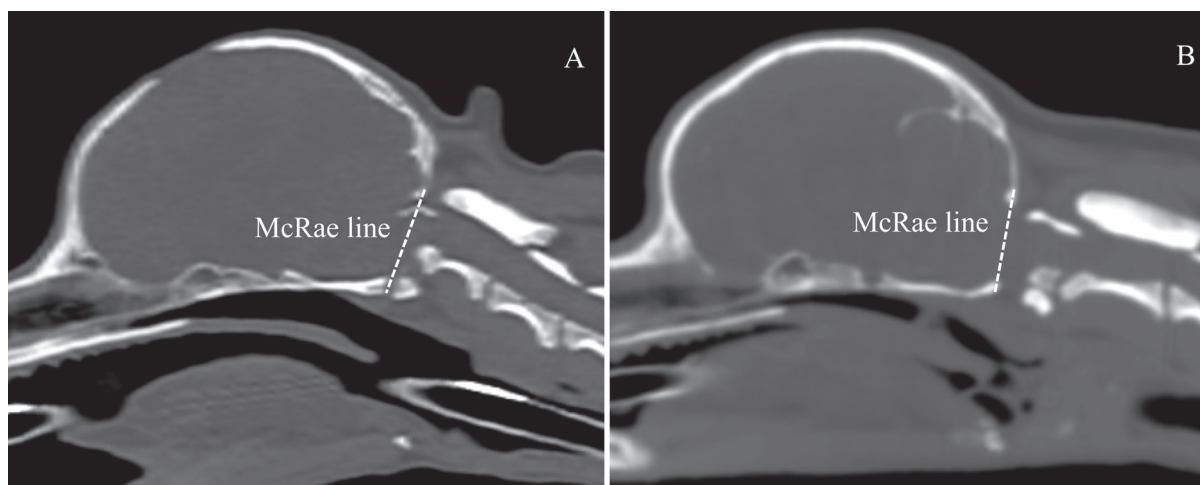


Fig. 1. Computed tomography images of dogs with (A) and without (B) atlantoaxial subluxation complicated by atlantooccipital overlapping (AOO). AOO was diagnosed using a three-dimensional multiplanar reconstruction of the midsagittal section to confirm whether the arcus dorsalis of the atlas was located closer to the cranial aspect of the occipital bone than to the straight line joining the opisthion and basion of the occipital bone (the McRae line).

MATERIALS AND METHODS

Selection criteria

A total of 61 dogs with AAI, who underwent ventral fixation between October 2007 and October 2015 in the Veterinary Medical Teaching Hospital at Nippon Veterinary and Life Science University or in YPC Tokyo Animal Orthopedic Surgery Hospital, were included in the current study. All dogs underwent preoperative head and neck magnetic resonance (MR) imaging and computed tomography (CT) examinations. In our previous study, 41 redundant cases were followed-up postoperatively for a minimum of 180 days [43], and the present study adopted a similar follow-up period. Preoperative CT images were surveyed for the presence of AOO, and dogs were then assigned to an AOO or a non-AOO group accordingly. The following information was recorded: breed, sex, age (in months), and body weight at the time of surgery. CT images were also used to evaluate the size of the FM, syringomyelia, CC, dorsal compression (DC), and the degree of enlargement of each cerebral ventricle.

Anesthetic protocol during magnetic resonance imaging and computed tomography

Each animal received a pre-anesthetic dose of atropine sulfate (0.05 mg/kg, subcutaneously; Mitsubishi Tanabe Pharma Co., Osaka, Japan) and, after 10 min of pre-oxygenation, anesthesia was induced with intravenous midazolam (0.02 mg/kg; Astellas Pharma Inc., Tokyo, Japan) and propofol (4–8 mg/kg; Fresenius Kabi Japan Co., Tokyo, Japan), followed by endotracheal intubation. Anesthesia was maintained with sevoflurane (2.5–3.0%; Mylan Pharma Co., Tokyo, Japan) in oxygen.

Computed tomography and morphological evaluation

Image acquisition was performed with an 80- and 160-slice CT Aquilion PRIME-TSX-303A (Toshiba Medical Systems Co., Otawara, Japan) at a scan speed of 0.5 sec, with slice thickness and slice intervals of 0.5 mm each. The position of the head and neck during image acquisition may affect the apparent extent of AOO [3, 4]; therefore, the animals were maintained in a prone position with neutral extension during the imaging process, which was performed under general anesthesia. Morphological assessment was performed with an open-source DICOM viewer image-processing software (OsiriX version 5.6, 32-bit; Pixmeo SARL, Bernex, Switzerland). The DICOM data obtained from the CT images of each animal were used to create a three-dimensional multiplanar reconstruction (3D-MPR) to evaluate the extent of AOO and the size of the FM. The 3D-MPR CT images were assessed under the conditions described by Parry *et al.* [34]: window width of 2500 Hounsfield units (HU) and window level of 500 HU. Using a 3D-MPR midsagittal section, AOO was defined when the arcus dorsalis of the atlas was located closer to the cranial aspect of the occipital bone than to the straight line joining the opisthion and basion of the occipital bone (the McRae line) (Fig. 1) [29]. The FM index was calculated as the ratio of the height to the maximum width of the FM (Fig. 2) to evaluate occipital dysplasia.

Magnetic resonance imaging and morphological evaluation

GE Signa EXCITE 3.0-T (GE Healthcare Japan Co., Ltd., Tokyo, Japan), an open MR imaging system with a vertical magnetic field, was used to obtain MR images. Following the CT examination, MR imaging was performed under general anesthesia; the dogs remained in the same position as during the CT examination. We acquired T2-weighted images under the following conditions: slice thickness=2.0 mm, slice interval=0.4 mm, repetition time=5,000 msec, echo time=85.1 msec. MR images were

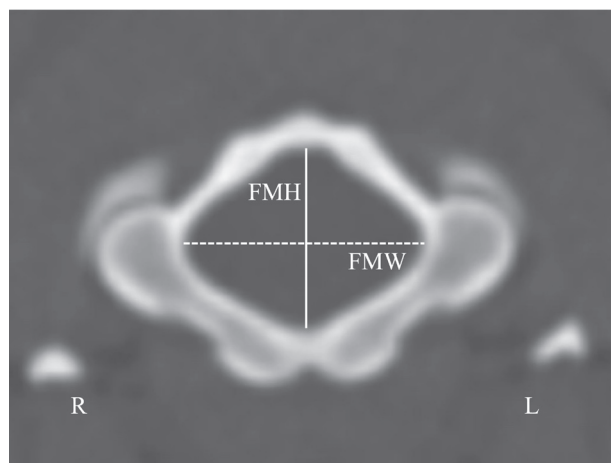


Fig. 2. Computed tomography images of the foramen magnum (FM) in a healthy beagle dog. The calculated FM index was the ratio of the height of the FM (FMH) to the maximum width of the FM (FMW). The maximum internal height of the FM and the maximum internal width of the FM were measured in a three-dimensional multiplanar reconstruction of the axial section.

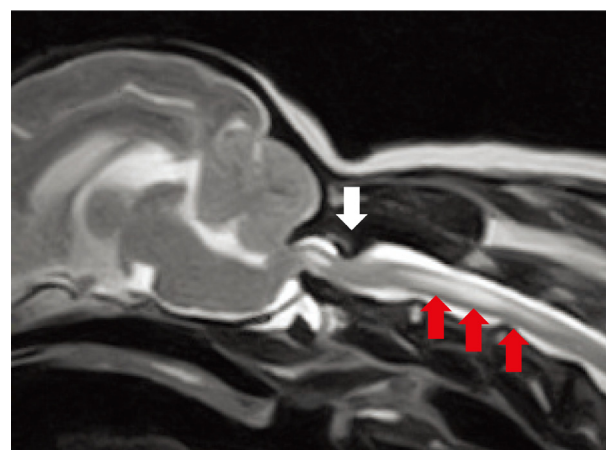


Fig. 3. A midsagittal cross-section of a T2-weighted magnetic resonance image of the head and neck of a dog with atlantoaxial instability, complicating syringomyelia, and dorsal compression. Syringomyelia was assessed only in the cervical spinal cord and was defined as dilatation of the central canal of the spinal cord (red arrows). Dorsal compression was defined as the compression of the spinal cord from the dorsal side in the atlantoaxial joint (white arrow).

morphologically assessed for the presence of syringomyelia, CC, and DC using the OsiriX DICOM viewer, and the CC index was measured [26]. Furthermore, the ratios of the height of the lateral ventricles to the height of the brain (VB ratio) [18], the height and width of the third ventricle (measured on the dorsal and ventral aspects of the interthalamic adhesion) to the height of the brain (TB ratio), the height of the fourth ventricle to the length of the cerebellum (FHC ratio), and the width of the fourth ventricle to the length of the cerebellum (FWC ratio) were evaluated. Syringomyelia was defined as dilatation of the central canal (Fig. 3). CC was defined as an indentation in the cerebellum in the midsagittal section of T2-weighted images of the head and neck [26]. The CC index was calculated according to the method outlined by Marino *et al.* (Fig. 4) [26]. DC was defined as the compression of the spinal cord from the dorsal side in the atlantoaxial joint in the midsagittal section of T2-weighted images of the head and neck (Fig. 3). The VB ratio, an index of dilatation of the lateral ventricles, was calculated at the level of the interthalamic adhesion in the transverse section of T2-weighted images of the head and neck (Fig. 5) [18]. When the left and right lateral ventricles differed in size, the height of the lateral ventricle was measured on the side with the greatest dilatation, where the ventricle was the most dilated in the ventrodorsal direction. In the current study, the TB ratio was determined to quantitatively assess the dilatation of the third ventricle (Fig. 6). The FHC and FWC ratios were calculated to assess dilatation of the fourth ventricle [22]. The FHC ratio was determined from the midsagittal section of a T2-weighted image of the head. The height of the fourth ventricle at the area of greatest dilatation in the ventrodorsal direction was divided by the maximum diameter of the cerebellum. The FWC ratio was obtained from the midsagittal section by dividing the distance between the anterior and posterior margins of the dorsal recess of the fourth ventricle by the maximum diameter of the cerebellum (Fig. 6).

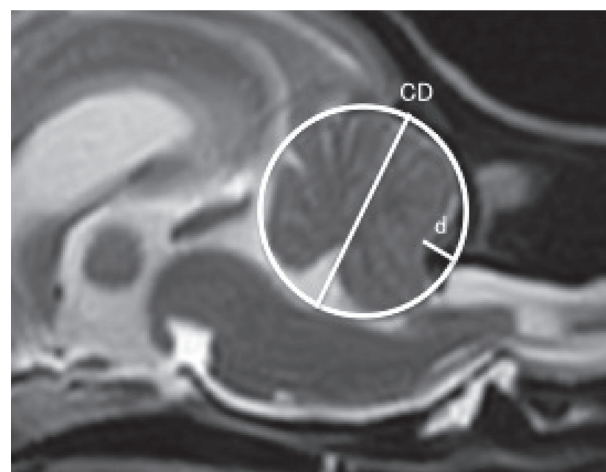


Fig. 4. A midsagittal cross-section of a T2-weighted magnetic resonance (MR) image of the head of a dog with atlantoaxial instability and complicating cerebellar compression. A circle formed by the maximum diameter (CD) of the cerebellum was traced in the midsagittal cross-section of the T2-weighted MR image. The distance (d) from the perimeter of the circle to the cerebellar parenchyma with the greatest compression was measured to determine the cerebellar compression index (cerebellar compression index = d/CD).

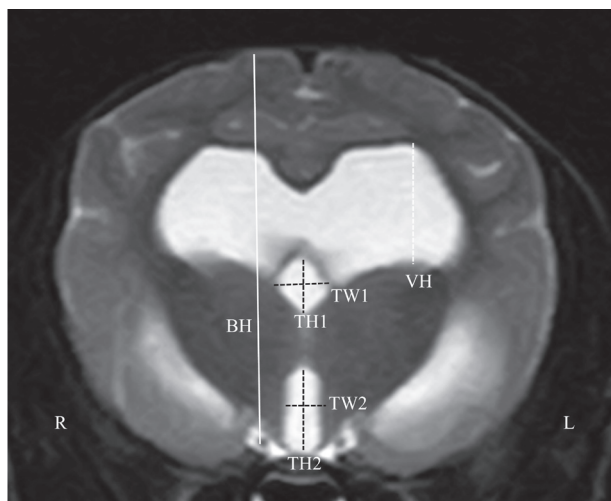


Fig. 5. Assessment of the height of the lateral ventricles and the maximum height and width of the third ventricle compared with the height of the brain using a T2-weighted magnetic resonance (MR) transverse image of the head of a dog. The measurements were made by calculating the ratio of the height of the lateral ventricles (VH) to the height of the brain (BH) at the level of the interthalamic adhesion in the T2-weighted MR transverse image of the head (VB ratio=VH/BH \times 100). The side with the greatest dilatation was used in cases of discrepancy between the left and right sides. The ratio of the sums of the maximum heights (TH1 and TH2) and maximum widths (TW1 and TW2) of the third ventricle (on the dorsal and ventral sides of the interthalamic adhesion) to BH was calculated at the level of the interthalamic adhesion in the transverse image (TB ratio=(TH1 + TH2 + TW1 + TW2)/BH \times 100).

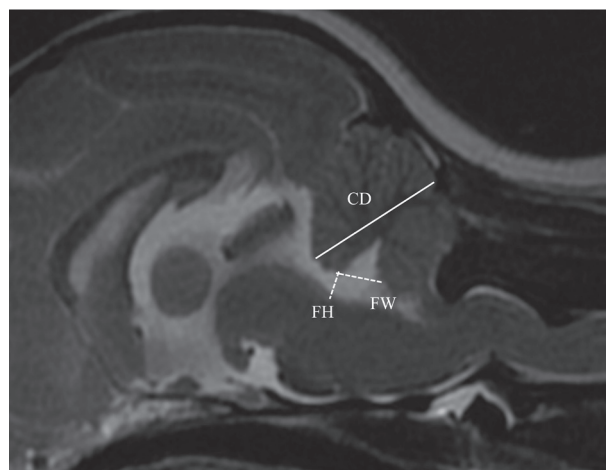


Fig. 6. Dilatation of the fourth ventricle measured using a midsagittal section of a T2-weighted magnetic resonance image of the head of a dog. The height of the fourth ventricle to the length of the cerebellum (FHC ratio) was determined when the height (FH) of the area of the greatest dilatation of the fourth ventricle in the ventrodorsal direction was divided by the maximum diameter of the cerebellum (CD) in the midsagittal section (FHC ratio=FH/CD \times 100). The width of the fourth ventricle to the length of the cerebellum (FWC ratio) was determined by dividing the distance (FW) between the anterior and posterior margins of the dorsal recess of the fourth ventricle by the CD (FWC ratio=FW/CD \times 100).

Statistical analyses

Statistical analyses were performed using the Statistical Package for the Social Sciences version 23 (IBM, Armonk, NY, U.S.A.). The Mann–Whitney *U* test or Student's *t*-test was used to assess differences between the AOO and non-AOO groups. Data are expressed as the mean \pm standard deviation (SD). Statistical significance was set at $P < 0.05$.

RESULTS

Signalment

Among the included 61 dogs, 23 were assigned to the AOO group, and 38 were assigned to the non-AOO group. The AOO group included 9 Yorkshire terriers, 9 Chihuahuas, 2 toy poodles, 1 Maltese, 1 shih tzu, and 1 mixed-breed dog. The non-AOO group comprised 13 Chihuahuas, 11 toy poodles, 5 Yorkshire terriers, 3 mixed-breed dogs, 2 miniature dachshunds, 2 Pomeranians, 1 cavalier King Charles spaniel, and 1 Japanese chin. Detailed information regarding sex was as follows: 8 sexually intact males, 5 castrated males, and 10 sexually intact females in the AOO group and 9 sexually intact males, 7 castrated males, 13 sexually intact females, and 9 spayed females in the non-AOO group. The mean age was 41.0 months (range, 5.0–127.0 months; median, 12.5 months; SD, 44.1 months) in the AOO group and 47.4 months (range, 5.0–143.0 months; median, 36.0 months; SD, 42.5 months) in the non-AOO group. The mean body weight was 2.0 kg (range, 0.9–4.3 kg; median, 1.8 kg; SD, 0.9 kg) in the AOO group and 2.5 kg (range, 1.2–9.0 kg; median, 2.3 kg; SD, 1.4 kg) in the non-AOO group. No significant differences in the mean age ($P = 0.332$) or body weight ($P = 0.060$) were observed between the AOO and the non-AOO groups at the time of surgery.

Foramen magnum index

The mean FM index was 1.45 (range, 1.15–1.96; median, 1.34; SD, 0.25) in the 23 dogs in the AOO group and 1.45 (range, 0.81–2.19; median, 1.39; SD, 0.38) in the 38 dogs in the non-AOO group. The mean FM index did not differ significantly between the two groups ($P = 0.852$; Table 1).

Syringomyelia

Syringomyelia was observed in 5 dogs in the AOO group and 9 dogs in the non-AOO group. The dogs with syringomyelia included 4 Yorkshire terriers and 1 Chihuahua in the AOO group and 4 Chihuahuas, 2 toy poodles, 1 Yorkshire terrier, 1

Table 1. The size of foramen magnum

	FM index			
	Mean	Range	Median	SD
AOO group	1.45	1.15–1.96	1.34	0.25
Non-AOO group	1.45	0.81–2.19	1.39	0.38

FM: foramen magnum, AOO: atlantooccipital overlapping, SD: standard deviation.

Table 2. Comparison of concurrent conditions

	Syringomyelia (%)	Cerebellar compression (%)	Dorsal compression (%)
AOO group	21.7 (5/23)	78.3 (18/23) ^a	8.7 (2/23)
Non-AOO group	23.7 (9/38)	34.2 (13/38) ^a	26.3 (10/38)

a) $P=0.001$. AOO: atlantooccipital overlapping.

Table 3. Ventricular dilatation

	VB ratio (%)				TB ratio (%)				FHC ratio (%)				FWC ratio (%)			
	Mean	Range	Median	SD	Mean	Range	Median	SD	Mean	Range	Median	SD	Mean	Range	Median	SD
AOO group	26.5 ^a	6.4–39.8	27.5	8.0	49.7	35.4–66.1	49.9	9.6	17.0 ^b	7.6–28.4	16.8	5.4	17.8 ^c	6.2–30.6	16.9	5.8
Non-AOO group	20.7 ^a	6.9–43.4	19.7	8.8	47.6	32.7–60.1	47.9	6.8	11.3 ^b	4.3–20.7	11.7	4.1	14.2 ^c	4.7–22.4	14.0	4.2

a) $P=0.011$, b) P =less than 0.001, c) $P=0.013$. VB: the height of the lateral ventricles to the height of the brain, TB: the height and width of the third ventricle to the height of the brain, FHC: the height of the fourth ventricle to the length of the cerebellum, FWC: the width of the fourth ventricle to the length of the cerebellum, SD: standard deviation.

Pomeranian, and 1 cavalier King Charles spaniel in the non-AOO group. The incidence of syringomyelia did not differ significantly between the two groups ($P=0.862$).

Cerebellar compression

CC was more common in the AOO group (18 of 23 dogs) than in the non-AOO group (13 of 38 dogs) ($P=0.001$; Table 2). The dogs with CC consisted of 9 Yorkshire terriers, 5 Chihuahuas, 2 toy poodles, 1 shih tzu, and 1 mixed-breed dog in the AOO group and 7 Chihuahuas, 2 toy poodles, 2 Yorkshire terriers, 1 cavalier King Charles spaniel, and 1 mixed-breed dog in the non-AOO group. The mean CC index was 11.4% (range, 7.4–22.6%; median, 10.3%; SD, 3.8%) in the affected 18 dogs in the AOO group and 10.6% (range, 4.6–20.2%; median, 10.0%; SD, 4.4%) in the 13 affected dogs in the non-AOO group.

Dorsal compression

DC was observed in 2 dogs in the AOO group and 10 dogs in the non-AOO group. The dogs with DC consisted of 1 Chihuahua and 1 Maltese in the AOO group and 7 Chihuahuas, 2 toy poodles, and 1 Yorkshire terrier in the non-AOO group. The incidence of DC did not differ significantly between the two groups ($P=0.096$).

Cerebral ventricle size

The VB ratio was significantly higher in the AOO group (mean, 26.5%; range, 6.4–39.8%; median, 27.5%; SD, 8.0%) than in the non-AOO group (mean, 20.7%; range, 6.9–43.4%; median, 19.7%; SD, 8.8%) ($P=0.011$). However, no significant difference in the TB ratio was found between the AOO group (mean, 49.7%; range, 35.4–66.1%; median, 49.9%; SD, 9.6%) and the non-AOO group (mean, 47.6%; range, 32.7–60.1%; median, 47.9%; SD, 6.8%) ($P=0.300$). The FHC ratio was significantly higher in the AOO group (mean, 17.0%; range, 7.6–28.4%; median, 16.8%; SD, 5.4%) than in the non-AOO group (mean, 11.3%; range, 4.3–20.7%; median, 11.7%; SD, 4.1%) ($P<0.001$). In addition, the FWC ratio was significantly higher in the AOO group (mean, 17.8%; range, 6.2–30.6%; median, 16.9%; SD, 5.8%) than in the non-AOO group (mean, 14.2%; range, 4.7–22.4%; median, 14.0%; SD, 4.2%) ($P=0.013$; Table 3).

DISCUSSION

The widespread use of MR imaging and CT in veterinary medicine has enabled the preoperative diagnosis of various forms of CJA, including AAI. However, the underlying pathophysiology of these abnormalities remains unclear; thus, effective treatments have not yet been established.

In previous studies [11, 18, 22], the degree of dilatation of the lateral ventricle has been evaluated using MR images. The

current study adopted the methodology employed by Kii *et al.* [18]. Flattening of the interthalamic adhesion and shrinkage of the suprasellar cistern have previously been used to assess dilatation of the third ventricle [22, 24, 38]; however, a quantitative method of assessment has not yet been established. Therefore, in the current study, we adopted the TB ratio as an index of third ventricle dilatation. Hasegawa *et al.* found that elderly dogs with cognitive disorders had brain atrophy and thin interthalamic adhesion [15]. If the size of interthalamic adhesion decreases with brain atrophy, ventriculomegaly involving the third ventricle may occur. However, none of the dogs included in this study experienced an epileptiform attack; therefore, we speculate that brain atrophy is less likely to affect the TB ratio. Previously, the maximum height of the fourth ventricle and the distance between the anterior and posterior margins of the dorsal recess of the fourth ventricle have been used to evaluate the dilatation of the fourth ventricle [22].

Occipital dysplasia has previously been defined as an abnormally large FM in an open-mouth rostral-caudal radiographic view of the head [1]. In recent years, improvement in imaging diagnosis technology in veterinary medicine has enabled the evaluation of the expansion of the FM because occipital dysplasia can be viewed in greater detail using CT rather than radiography. The FM index, an index of the size of the FM, is calculated by measuring the maximum width and height of the FM in a CT image or frame specimen of the head [16, 25, 32, 41].

The incidence of AOO is relatively high in Yorkshire terriers. Dogs with AOO may have secondary syringomyelia and hydrocephalus because of disturbances in CSF circulation in the junction between the medulla oblongata and the cervical spine [3–5, 8]. Cerda-Gonzalez *et al.* [4] found that among 4 dogs affected with AOO, all exhibited occipital dysplasia, 2 had ventriculomegaly, and 3 showed syringomyelia. In addition, Cerda-Gonzalez *et al.* [3] demonstrated that the incidence of syringomyelia was significantly higher ($P=0.0053$) in AOO-affected dogs (20/71) than in non-AOO-affected dogs (9/82). In the present study, the incidence of syringomyelia did not differ significantly between the AOO (5/23 dogs) and non-AOO groups (9/38 dogs) ($P=0.862$). A study on syringomyelia in cavalier King Charles spaniels indicated that the central canal had a diameter of ≥ 2 mm, as measured on transverse MR images [37]. However, considering the differences in the central canal in different sizes of dogs, this measurement would be difficult to perform in small dog breeds. In the present study, syringomyelia was defined as clear dilatation of the central canal in MR images.

Significantly greater dilatation of the lateral ventricles and the fourth ventricle was observed in the AOO group than in the non-AOO group. In humans, the lateral ventricles are less compliant than the third and fourth ventricles and have the greatest change in pressure relative to the change in volume [20]. In the current study, the dogs in the AOO group did not show dilatation in the third ventricle despite major dilatation in the lateral ventricles and the fourth ventricle, suggesting different compliance in these ventricles. The lateral and fourth ventricles were significantly more dilated (VB ratio, $P=0.011$; FHC ratio, $P<0.001$; FWC ratio, $P=0.013$) in the presence of concurrent AOO, which might have induced secondary arachnoiditis around the atlantooccipital joint or displacement of the cerebellum. Arachnoiditis may consequently have caused partial blockage of CSF flow at the foramen of Luschka, where the CSF drains from the fourth ventricle into the subarachnoid space. The significantly higher rate of CC observed in the AOO group suggests that blockage of CSF flow at the foramen of Luschka caused by displacement of the cerebellum may have contributed to the dilatation of the lateral and fourth ventricles. Notably, a relatively high incidence of AOO was observed in the Yorkshire terriers; thus, it is possible that skull shape affects cerebral ventricle size and the incidence of CC.

The FM index in the current study did not differ significantly between the AOO group and the non-AOO group, and CC was observed in 34.2% of dogs in the non-AOO group, suggesting the presence of latent AOO and atlantooccipital instability (AOI). AOO is a dynamic lesion, the underlying mechanism of which is poorly understood, although its association with AOI has been noted [4]. Rotation of the atlas relative to the occipital condyle is commonly observed in dogs with AOO or AOI [14, 39, 42]. When AOI is caused by a defect in the occipital condyle, a strangulated lesion may be present in the junction between the medulla oblongata and spinal cord. Excessive joint mobility and compression of the articular facets have been implicated in fibrosis around the atlantooccipital joint [6, 31]. A fibrous band on the caudal surface of the FM, believed to be synonymous with a strangulated lesion, has been implicated in syringomyelia [3, 4]. Previous studies in humans and dogs with Chiari-like malformations have suggested that fibrous bands within the atlantooccipital and atlantoaxial joints impair CSF circulation [3, 4, 6, 31]. AOO can result in the formation of a dural band owing to the excessive motion of the atlas relative to the occipital bone [3, 4]. Therefore, AOO and AOI are related to dysplasia of the atlantooccipital joint. In cases of concurrent AAI, stabilization of the atlantoaxial joint also has the potential to limit excessive mobility of the atlantooccipital joint.

In this study, the height of the brain and the maximum diameter of the cerebellum of each dog were investigated to account for inter-breed differences, and every cerebral ventricle was also examined. Furthermore, occipital dysplasia is a condition frequently observed in toy breeds and small dogs [4]. In the present study, because the FM index did not differ significantly between the AOO and non-AOO groups, occipital dysplasia is unlikely to have affected the cerebral ventricle size in the dogs with AAI. Previous studies have indicated that occipital dysplasia alone does not cause neurological abnormalities [33, 46]. Furthermore, similarly to patients with BI [19], dogs are more likely develop cranial displacement of the atlas toward the FM when occipital dysplasia is present [3, 4]. Reported causes of BI in humans include congenital skull dysplasia and pathological softening of the bone [28, 35]. Canine AOO may involve congenital skull dysplasia resulting from a connective tissue abnormality [4]. BI in humans can lead to hypoplasia of the occipital condyle, an irregularly-shaped occipital condyle, and dysplasia of the atlantooccipital joint [13, 36]. Dogs with inadequate calcification of the skull may develop dysplasia, whereby the axial muscles cause a compressive force between the skull and cervical spine, pushing the atlantooccipital joint into the skull. In the current study, the dogs in the non-AOO group tended to have a higher incidence of DC than did those in the AOO group. In the absence of AOO, bending and stretching of the head affect the atlantoaxial joint, and compensatory thickening of the ligamentum flavum occurs. By contrast, in cases of complicating AOO, bending and stretching of the head may be associated with excessive mobility of the atlantooccipital joint.

Therefore, the load to the unstable atlantoaxial joint becomes smaller in cases with complicating AOO than in cases without AOO.

A few limitations of the present study must be noted. First, because the head and neck were not positioned at maximum extension during imaging, AOO may have gone undetected in the dogs in the non-AOO group. This study was intended to investigate AAI-affected dogs. Excessive extending or flexing of the head and neck during imaging risks iatrogenic damage to the spinal cord. Therefore, the dogs were maintained in a prone position with neutral extension during the imaging, which was performed under general anesthesia. However, the position of the head and neck at the time of imaging may have affected CSF circulation. Second, the implants used for ventral fixation of the atlantoaxial joint were composed of stainless steel; thus, MR imaging for postoperative evaluation was impossible. However, implants composed of titanium would have enabled postoperative MR imaging evaluation of AAI and disturbances in CSF circulation would have been fully assessed. Third, no comprehensive studies have detailed normal ventricular size in toy breeds; therefore, the ventricle size may be variable in non-pathological conditions.

In summary, this study investigated the cerebral ventricle size and concurrent CJA, which were identified in preoperative MR and CT images, in dogs with AAI that underwent ventral fixation in AOO and non-AOO groups. Dogs with concurrent AOO exhibited significantly more dilatation of the lateral and fourth ventricles.

CONFLICTS OF INTEREST. No third-party funding or support was received for this study or for the writing and publication of this manuscript. The authors have no conflicts of interest to declare.

REFERENCES

1. Bagley, R. S. 2005. Options for diagnostic testing in animals with neurologic disease. pp. 207–238. *In: Fundamentals of Veterinary Clinical Neurology*, 1st ed., Blackwell Publishing, Ames.
2. Beaver, D. P., Ellison, G. W., Lewis, D. D., Goring, R. L., Kubilis, P. S. and Barchard, C. 2000. Risk factors affecting the outcome of surgery for atlantoaxial subluxation in dogs: 46 cases (1978–1998). *J. Am. Vet. Med. Assoc.* **216**: 1104–1109. [[Medline](#)] [[CrossRef](#)]
3. Cerda-Gonzalez, S., Bibi, K. F., Gifford, A. T., Mudrak, E. L. and Scrivani, P. V. 2016. Magnetic resonance imaging-based measures of atlas position: Relationship to canine atlantooccipital overlapping, syringomyelia and clinical signs. *Vet. J.* **209**: 133–138. [[Medline](#)] [[CrossRef](#)]
4. Cerda-Gonzalez, S., Dewey, C. W., Scrivani, P. V. and Kline, K. L. 2009. Imaging features of atlanto-occipital overlapping in dogs. *Vet. Radiol. Ultrasound* **50**: 264–268. [[Medline](#)] [[CrossRef](#)]
5. Cerda-Gonzalez, S. and Dewey, C. W. 2010. Congenital diseases of the craniocervical junction in the dog. *Vet. Clin. North Am. Small Anim. Pract.* **40**: 121–141. [[Medline](#)] [[CrossRef](#)]
6. Chamberlain, W. E. 1939. Basilar impression (Platybasia): a bizarre developmental anomaly of the occipital bone and upper cervical spine with striking and misleading neurologic manifestations. *Yale J. Biol. Med.* **11**: 487–496. [[Medline](#)]
7. Denny, H. R., Gibbs, C. and Waterman, A. 1998. Atlanto-axial subluxation in the dog: a review of thirty cases and an evaluation of treatment by lag screw fixation. *J. Small Anim. Pract.* **29**: 37–47. [[CrossRef](#)]
8. Dewey, C. W., Marino, D. J. and Loughin, C. A. 2013. Craniocervical junction abnormalities in dogs. *N. Z. Vet. J.* **61**: 202–211. [[Medline](#)] [[CrossRef](#)]
9. Downey, R. S. 1967. An unusual cause of tetraplegia in a dog. *Can. Vet. J.* **8**: 216–217. [[Medline](#)]
10. Erbenli, A. and Oge, H. K. 1994. Congenital malformations of the craniovertebral junction: classification and surgical treatment. *Acta Neurochir. (Wien)* **127**: 180–185. [[Medline](#)] [[CrossRef](#)]
11. Esteve-Ratsch, B., Kneissl, S. and Gabler, C. 2001. Comparative evaluation of the ventricles in the Yorkshire Terrier and the German Shepherd dog using low-field MRI. *Vet. Radiol. Ultrasound* **42**: 410–413. [[Medline](#)] [[CrossRef](#)]
12. Geary, J. C., Oliver, J. E. and Hoerlein, B. F. 1967. Atlanto axial subluxation in the canine. *J. Small Anim. Pract.* **8**: 577–582. [[Medline](#)] [[CrossRef](#)]
13. Goel, A. 1999. Chiari I malformation redefined: clinical and radiographic findings for 364 symptomatic patients. *Neurosurgery* **45**: 1497–1499. [[Medline](#)] [[CrossRef](#)]
14. Greenwood, K. M. and Oliver, J. E. Jr. 1978. Traumatic atlanto-occipital dislocation in two dogs. *J. Am. Vet. Med. Assoc.* **173**: 1324–1327. [[Medline](#)]
15. Hasegawa, D., Yayoshi, N., Fujita, Y., Fujita, M. and Orima, H. 2005. Measurement of interthalamic adhesion thickness as a criteria for brain atrophy in dogs with and without cognitive dysfunction (dementia). *Vet. Radiol. Ultrasound* **46**: 452–457. [[Medline](#)] [[CrossRef](#)]
16. Janeczek, M., Chrószcz, A., Onar, V., Pazvant, G. and Pospieszny, N. 2008. Morphological analysis of the foramen magnum of dogs from the Iron Age. *Anat. Histol. Embryol.* **37**: 359–361. [[Medline](#)] [[CrossRef](#)]
17. Johnson, S. G. and Hulse, D. A. 1989. Odontoid dysplasia with atlantoaxial instability in a dog. *J. Am. Anim. Hosp. Assoc.* **25**: 400–404.
18. Kii, S., Uzuka, Y., Taura, Y., Nakaichi, M., Takeuchi, A., Inokuma, H. and Onishi, T. 1997. Magnetic resonance imaging of the lateral ventricles in beagle-type dogs. *Vet. Radiol. Ultrasound* **38**: 430–433. [[Medline](#)] [[CrossRef](#)]
19. Kim, F. M. 2000. Developmental anomalies of the craniocervical junction and cervical spine. *Magn. Reson. Imaging Clin. N. Am.* **8**: 651–674. [[Medline](#)]
20. Kimura, M., Tamaki, N., Kose, S., Takamori, T. and Matsumoto, S. 1989. Computer simulation of intracranial pressure using electrical R-C circuit. pp. 295–298. *In: Intracranial Pressure VII* (Hoff, J. T. and Betz, A. L. eds), Springer, Berlin, Heidelberg.
21. Ladds, P., Guffy, M., Blauch, B. and Splitter, G. 1971. Congenital odontoid process separation in two dogs. *J. Small Anim. Pract.* **12**: 463–471. [[Medline](#)] [[CrossRef](#)]
22. Laubner, S., Ondreka, N., Failing, K., Kramer, M. and Schmidt, M. J. 2015. Magnetic resonance imaging signs of high intraventricular pressure—comparison of findings in dogs with clinically relevant internal hydrocephalus and asymptomatic dogs with ventriculomegaly. *BMC Vet. Res.* **11**: 181. [[Medline](#)] [[CrossRef](#)]
23. Levine, D. N. 2004. The pathogenesis of syringomyelia associated with lesions at the foramen magnum: a critical review of existing theories and proposal of a new hypothesis. *J. Neurol. Sci.* **220**: 3–21. [[Medline](#)] [[CrossRef](#)]
24. MacKillop, E. 2011. Magnetic resonance imaging of intracranial malformations in dogs and cats. *Vet. Radiol. Ultrasound* **52** Suppl 1: S42–S51.

- [\[Medline\]](#) [\[CrossRef\]](#)
25. Madadin, M., Menezes, R. G., Al Saif, H. S., Abu Alola, H., Al Muhanna, A., Gullenpet, A. H., Nagesh, K. R., Kharoshah, M. A. and Al Dhafery, B. 2017. Morphometric evaluation of the foramen magnum for sex determination: A study from Saudi Arabia. *J. Forensic Leg. Med.* **46**: 66–71. [\[Medline\]](#) [\[CrossRef\]](#)
26. Marino, D. J., Loughin, C. A., Dewey, C. W., Marino, L. J., Sackman, J. J., Lesser, M. L. and Akerman, M. B. 2012. Morphometric features of the craniocervical junction region in dogs with suspected Chiari-like malformation determined by combined use of magnetic resonance imaging and computed tomography. *Am. J. Vet. Res.* **73**: 105–111. [\[Medline\]](#) [\[CrossRef\]](#)
27. McCarthy, R. J., Lewis, D. D. and Hosgood, G. 1995. Atlantoaxial luxation in dogs. *Comp. Contin. Educ. Pract.* **17**: 215–226.
28. McGREGOR, M. 1948. The significance of certain measurements of the skull in the diagnosis of basilar impression. *Br. J. Radiol.* **21**: 171–181. [\[Medline\]](#) [\[CrossRef\]](#)
29. McRae, D. L. and Barnum, A. S. 1953. Occipitalization of the atlas. *Am. J. Roentgenol. Radium Ther. Nucl. Med.* **70**: 23–46. [\[Medline\]](#)
30. Milhorat, T. H., Capocelli, A. L. Jr., Anzil, A. P., Kotzen, R. M. and Milhorat, R. H. 1995. Pathological basis of spinal cord cavitation in syringomyelia: analysis of 105 autopsy cases. *J. Neurosurg.* **82**: 802–812. [\[Medline\]](#) [\[CrossRef\]](#)
31. Nakamura, N., Iwasaki, Y., Hida, K., Abe, H., Fujioka, Y. and Nagashima, K. 2000. Dural band pathology in syringomyelia with Chiari type I malformation. *Neuropathology* **20**: 38–43. [\[Medline\]](#) [\[CrossRef\]](#)
32. Onar, V., Mutuş, R. and Kahvecioğlu, K. O. 1997. Morphometric analysis of the foramen magnum in German shepherd dogs (Alsations). *Ann. Anat.* **179**: 563–568. [\[Medline\]](#) [\[CrossRef\]](#)
33. Parker, A. J. and Park, R. D. 1974. Occipital dysplasia in the dog. *J. Am. Anim. Hosp. Assoc.* **10**: 520–525.
34. Parry, A. T., Upjohn, M. M., Schlegl, K., Kneissl, S. and Lamb, C. R. 2010. Computed tomography variations in morphology of the canine atlas in dogs with and without atlantoaxial subluxation. *Vet. Radiol. Ultrasound* **51**: 596–600. [\[Medline\]](#) [\[CrossRef\]](#)
35. Pearce, J. M. 2007. Platybasia and basilar invagination. *Eur. Neurol.* **58**: 62–64. [\[Medline\]](#) [\[CrossRef\]](#)
36. Rao, P. V., Mbajorgu, E. F. and Levy, L. F. 2002. Bony anomalies of the craniocervical junction. *Cent. Afr. J. Med.* **48**: 17–23. [\[Medline\]](#)
37. Rusbridge, C., Greitz, D. and Iskandar, B. J. 2006. Syringomyelia: current concepts in pathogenesis, diagnosis, and treatment. *J. Vet. Intern. Med.* **20**: 469–479. [\[Medline\]](#) [\[CrossRef\]](#)
38. Ryan, C. T., Glass, E. N., Seiler, G., Zwingenberger, A. L. and Mai, W. 2014. Magnetic resonance imaging findings associated with lateral cerebral ventriculomegaly in English Bulldogs. *Vet. Radiol. Ultrasound* **55**: 292–299. [\[Medline\]](#) [\[CrossRef\]](#)
39. Rylander, H. and Robles, J. C. 2007. Diagnosis and treatment of a chronic atlanto-occipital subluxation in a dog. *J. Am. Anim. Hosp. Assoc.* **43**: 173–178. [\[Medline\]](#) [\[CrossRef\]](#)
40. Shores, A. and Tepper, L. C. 2007. A modified ventral approach to the atlantoaxial junction in the dog. *Vet. Surg.* **36**: 765–770. [\[Medline\]](#) [\[CrossRef\]](#)
41. Simoens, P., Poels, P. and Lauwers, H. 1994. Morphometric analysis of the foramen magnum in Pekingese dogs. *Am. J. Vet. Res.* **55**: 34–39. [\[Medline\]](#)
42. Steffen, F., Flueckiger, M. and Montavon, P. M. 2003. Traumatic atlanto-occipital luxation in a dog: associated hypoglossal nerve deficits and use of 3-dimensional computed tomography. *Vet. Surg.* **32**: 411–415. [\[Medline\]](#) [\[CrossRef\]](#)
43. Takahashi, F., Hakozaiki, T., Kouno, S., Suzuki, S., Sato, A., Kanno, N., Harada, Y., Yamaguchi, S. and Hara, Y. 2018. Atlantooccipital overlapping and its effect on outcomes after ventral fixation in dogs with atlantoaxial instability. *J. Vet. Med. Sci.* **80**: 526–531. [\[Medline\]](#) [\[CrossRef\]](#)
44. Thomas, W. B., Sorjonen, D. C. and Simpson, S. T. 1991. Surgical management of atlantoaxial subluxation in 23 dogs. *Vet. Surg.* **20**: 409–412. [\[Medline\]](#) [\[CrossRef\]](#)
45. Watson, A. G. and de Lahunta, A. 1989. Atlantoaxial subluxation and absence of transverse ligament of the atlas in a dog. *J. Am. Vet. Med. Assoc.* **195**: 235–237. [\[Medline\]](#)
46. Zaki, F. A. 1980. Odontoid process dysplasia in a dog. *J. Small Anim. Pract.* **21**: 227–234. [\[Medline\]](#) [\[CrossRef\]](#)